LANGMUIR

pubs.acs.org/Langmuir Article

Dynamics of Confined Microgel Liquids: Weakened Spatial Confinement Effect by Microgel Particle Compliance

Raymond P. Seekell, III, Kehua Lin, and Yingxi Zhu*

Cite This: https://doi.org/10.1021/acs.langmuir.1c00363 Read Online

ACCESS | Metrics & More | Article Recommendations | Supporting Information

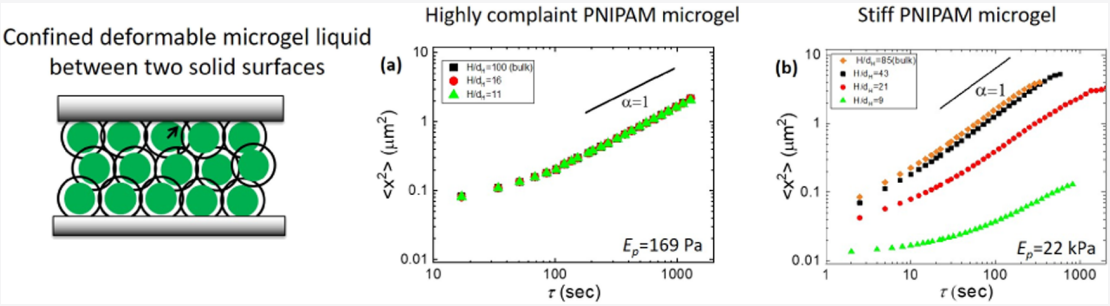

ABSTRACT: Spatial confinement has a great impact on the structures and dynamics of interfacial molecular and polymer liquid films. Most prior research has focused on confined liquids of fixed material compliance and often treated them in approximation to the "hard-sphere" interaction model. In this study, we microscopically investigate the structural dynamics of highly deformable poly(*N*-isopropylacrylamide) (PNIPAM) microgels confined between two solid surfaces in comparison to that of nearly nondeformable microgels of the same chemistry. We observe that the mobility and structural relaxation of highly deformable PNIPAM microgels at an apparent volume fraction, ϕ = 0.49−0.70, show little change with the reduction of gap spacing, in stark contrast to confinement-induced dynamic retardation of "hard-sphere"-like stiff PNIPAM microgels. The critical gap spacing, defined as the onset of confinement effect to deviate from the bulk behavior, is found to be approximately 17−22 particle layers for highly deformable microgels of ϕ = 0.56−0.70, much smaller than that of approximately 40 particle layers or larger for stiff microgels or model "hard-sphere" colloidal liquids of similar ϕ. Additionally, we observe no evident confinement-enhanced structural reorganization of deformable microgels near the confining surfaces when gap spacing approaches the critical gap spacing. Microgel deformation upon strong confinement is attributed to the disrupted confinement-induced ordering of confined microgels. Hence, it is clearly indicated that spatial confinement exhibits a much weaker effect on highly compliant microgel particles than stiff ones, resulting in a negligible to moderate reduction in microgel interfacial dynamics. It therefore gives insights into the molecular design of polymeric thin films of variable compliance to control friction and lubrication.

■ INTRODUCTION

The effect of spatial confinement on the structure and dynamics of liquids has been studied over the past several decades.[1−7] It has been much reported that spatial confinement can effectively modify the packing structure, dynamic process, and even phase behavior of molecular and macromolecular liquids.[1,4,8−14] For many molecular and macromolecular liquids, dimensional spatial reduction could significantly impede structural relaxation and slowdown their dynamics under constant temperature and volume fraction conditions. When the gap spacing between two flat confining surfaces is reduced to be comparable to, or less than, molecular or particle dimensions, an increasingly ordered structure of confined liquids relative to the bulk state is observed, where molecules or particles assemble into discrete layers parallel to these surfaces. As a result, the effective shear viscosities, diffusion rates, and relaxation times of these confined liquids increase significantly.[13−17] Spatial confinement has, therefore, a great impact on controlling the structural and dynamics of complex thin films for various industrial applications ranging from coating, lubrications, to soft lithography.

Confined simple liquids are often modeled as "hard-sphere" liquids with noncompliant and constant molecular dimension and exhibit wall-induced structuring and modified interfacial dynamics from their bulk behaviors. However, for many complex materials, such as polymer gels and biomacromolecular aggregates, their dimension and shape can be largely tuned by external pressure due to their interpenetrable

Received: February 6, 2021
Revised: April 6, 2021

polymer network, giving rise to different short-ranged interparticle interactions from "hard-sphere" repulsion.[1,4,5,7,13,14,17] Accordingly, these complex materials upon confinement could exhibit some intriguing and unique interfacial structures and dynamics. For instance, synovial fluids, which are the aggregates of hyaluronic acid polymers with lubricin protein in mammalian articular joints, exhibit long-lasting ultralow friction upon confinement between cartilage surfaces.[18−21] Also, recent studies of deformable microgels have reported a frustrated packing configuration of confined microgel monolayers,[22] deformation-induced vanishing of yielding stress,[23] and interfacial slip flow of dense microgel liquids near solid surfaces.[3,24−26] However, a direct comparative study of how particle compliance impacts the structure and dynamics of confined liquids of the same chemistry yet varied compliance seems sparse, despite its significance in understanding the mechanism of superlubrication and molecular design of advanced lubricious materials and coatings.

In recent years, colloidal liquids have been used to model molecular liquids to allow direct experimental investigation of their structures and dynamics thanks to their observable sizes by different microscopic methods, such as wide-field microscopy and confocal laser scanning microscopy (CLSM).[5,27−29] It has been confirmed that the dynamics of bulk and confined colloidal liquids could resemble the behaviors of bulk and confined molecular liquids, respectively.[5,28,29] Spatial confinement could cause significant dynamic retardation of model "hard-sphere" colloidal liquids, such as poly(methyl methacrylate) (PMMA) microspheres suspended in density and index-of-reflection matched liquids of varied particle volume fractions, ϕ = 0.40−0.57.[5,28,29] Moreover, glass-like dynamics is observed when the gap spacing between confining surfaces is reduced to the thickness of 10−60 particle layers.[5,28,29] Critical gap spacing, where dynamic arrest commences, is found to be in the range of 40−60 particle layers with strongly ϕ-dependence for "hard-sphere" PMMA colloidal liquids.[30] On the other side, it is intriguingly reported that the glass-like behaviors of dense colloidal liquids could be modified by varying cross-linking density of microgel particles, leading to varied particle compliance.[31−34] For highly compliant microgels in suspensions, dynamic interparticle bonding, resulting from particle deformation, could give rise to anisotropic elastic interparticle interaction. As a result, increased particle compliance or deformability has led to the shift of glass transition to a higher volume fraction in comparison to model "hard-sphere" colloidal dense liquids, suggesting enhanced structural relaxation with a delayed glass behavior.[32−34] Thus, it is of great interest to directly examine the impact of spatial confinement on the dynamic behavior of highly compliant microgels in comparison to confined "hard-sphere" liquids by direct microscopic observation.

In this study, we examine the effect of spatial confinement on the structural dynamics of microgel liquids of the same chemistry but distinct particle compliance by using a custom-made compression apparatus integrated with CLSM. Specifically, we focus on fluorescence-labeled poly(*N*-isopropylacrylamide) (PNIPAM) microgel particles of two different cross-linking densities, which yield distinct compliance of microgel particles, designed one as a deformable microgel and the other one as stiff one resembling model "hard-sphere" liquids.[32,34] We investigate the dependence of particle mobility and structural relaxation of confined PNIPAM microgel liquids of varied microgel concentrations between two solid surfaces of varied gap spacings over the range from the bulk (greater than 100 particle layers) to ∼10 particle layers. At each incremental gap spacings, the structural dynamics of confined microgel liquids is characterized by CLSM in real-space and real-time image analysis at a single particle resolution. We thereby quantify the variance of critical gap spacing for the onset of spatial confinement against microgel particle compliance.

■ EXPERIMENTAL SECTION

Materials. Fluorescence-labeled PNIPAM microgels were synthesized using a method of free radical polymerization described previously,[32,35] for which methylene-bis-acrylamide (BIS) was used as the cross-linker. In this work, we focus on two PNIPAM microgels of contrasting stiffness by varying cross-linking density (CL) based on the mass ratio of the BIS cross-linker to *N*-isopropylacrylamide (NIPAM) monomer, $\mathrm{CL} = \frac{[\mathrm{BIS}]}{[\mathrm{BIS}] + [\mathrm{NIPAM}]}$ = 1.6 and 6.0%. The particle elasticity, E_p, of PNIPAM microgels of CL = 1.6 and 6.0% was measured to be 169 ± 24 Pa and 22 ± 0.15 kPa by analyzing osmotic pressure-dependent particle size change with a simple Hertzian model.[36] In our previous study of dense PNIPAM microgels of varied CL, we have ranked the microgels of CL = 0.9−6.6% from highly deformable particles to "hard-spheres"-like ones, respectively.[32] In this work, we examined the dynamics of confined PNIPAM microgels of E_p = 169 Pa and 22 kPa to understand the effect of microgel particle stiffness on the structural relaxation of confined liquids.[32] Dense PNIPAM microgels of apparent volume fraction, ϕ = 0.49−0.70, in water were prepared by concentrating the microgel suspensions using a Rotovap R-210 at 60 °C and rediluting with deionized water.

Characterization. A home-built compression apparatus integrated with CLSM was employed to study the structure and dynamics of confined PNIPAM thin films between two optical-smooth quartz solid surfaces of varied thicknesses. As schematically shown in Supporting Information Figure S1a, the compression apparatus is mounted on the sample stage of an inverted confocal laser scanning microscope (Cal Zeiss LSM 5 Pa) with an oil-immersion objective lens (NA = 1.4, 100×) to allow three-dimensional visualization of confined PNIPAM microgel particles in aqueous suspensions. To reduce the depletion of PNIPAM from smooth quartz surfaces, a thin layer of nonfluorescent polydispersed PNIPAM microgels of CL = 6.0% and several microns in diameter was spin-coated onto the quartz coverslips and sintered at 80 °C to roughen both confining surfaces. It helped prevent localized crystallization of confined PNIPAM microgels between two surfaces.

A PNIPAM microgel suspension at a given volume fraction was loaded into the compressible sample cell using a pipet and sealed with UV-curing glue. Desired gap spacing was obtained by lowering the top surface toward the bottom one in a stepwise fashion using two coarse micrometers of 1 μm in resolution and one fine micrometer of 0.1 μm that is an order of magnitude smaller than PNIPAM microgel diameter of 1.5−2.5 μm. The parallel layer between the top and bottom surfaces was tuned by the fine micrometer and examined by the uniform fluorescence intensity across the microscopic scan area of microgel layers immediately adjacent to the top and bottom surfaces. The gap spacing was decreased at a typical compression rate of ∼10 μm/min, and waited for a time period of ∼5 min between each compression step to minimalize the mechanical drift. Typically, the first image acquisition was performed at a large gap size to capture the bulk behavior, and the top solid surface was lowered to incremental smaller gap spacings before each subsequent measurement. The film thickness of confined PNIPAM microgels was determined by the confocal z-stack profiles with an accuracy of ±0.2 μm, thanks to the nearly matching refractive index of PNIPAM microgels containing >95 wt % water to that of aqueous medium, which was also confirmed by the travel distance of the fine micrometer. It is noted that the smallest gap spacing controlled in this work is approximately 9−10 particle layers, considering the nonfluorescent PNIPMA coating and strong microgel particle−surface interaction. After a gap spacing is

https://doi.org/10.1021/acs.langmuir.1c00363
Langmuir XXXX, XXX, XXX−XXX

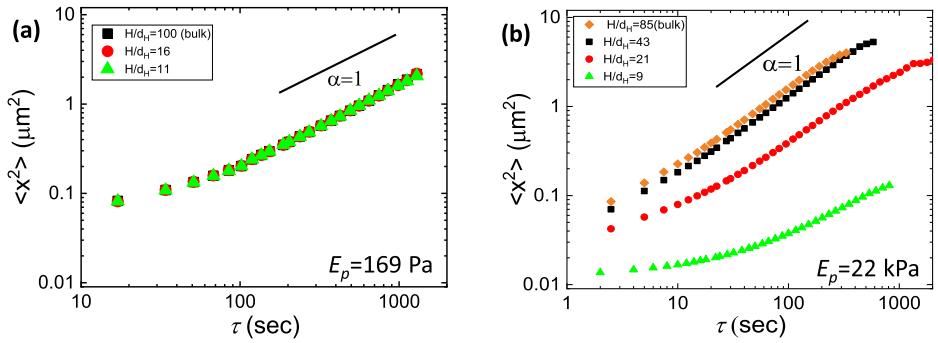

Figure 1. MSD against the lag time for confined PNIPAM microgels of E_p= (a) 169 Pa and (b) 22 kPa at ϕ = 0.49 against varied gap spacings, H/d_H, as denoted in each panel.

achieved, the sample was left undisturbed for ∼30 min before commencing measurements. All the measurements were performed at room temperature, T = 25 °C, where the microgels are swollen in aqueous suspensions. It is also noted that because of a high water content (>95 wt %) in PNIPAM microgel particles, the microgel liquids are nearly density matched. Thus, the gravity-induced sedimentation of confined PNIPAM microgel liquids is negligible. In this reported work, we also cautiously verified the volume fraction of each layers of confined microgel liquids upon the completion of each experiment to be the same as the initial ones within experimental uncertainty.

Z-stack and time (t)-dependent image analyses were accomplished using the IDL particle-tracking algorithms as detailed elsewhere.[5,37,38] Three-dimensional z-stack images were acquired over a scanning area of 30 μm × 30 μm in the $x-y$ plane, while the scanning height in the z-direction varied with gap spacing. To mitigate the wall effects, we focused on the dynamics of microgel particles confined at the midplane of the confined microgel thin film. At bulk and large gap spacings, the image size in the z-direction was chosen to be 12 μm. At smaller gap spacings, the size was reduced accordingly to ensure that the particles in acquired images were at least 2 particle layers from each confining surface, which thereby limited us to keep the gap spacing of ∼9−10 particle layers or thicker in this work. All confined microgel particles in aqueous suspensions exhibited disordered structures as a representative fluorescence micrograph is shown in Supporting Information Figure S1b. Particle centroid-finding algorithms were employed to identify particle positions and obtain the trajectories of ∼1000 particles for all the images acquired in varied time series. We identified particle position with an accuracy of 0.05 μm in the $x-y$ plane and 0.2 μm in the z-direction.

The structure of confined microgel liquids at varied volume fractions and gap spacings was analyzed by computing the pair correlation function as

$$\int_0^\infty 4\pi r^2 \rho g(r) \mathrm{d}r = N \tag{1}$$

where r is the radial distance from the center of the particle, ρ is the number density of particles, and N is the total number of particles in the image-acquired sample. The dynamics of confined microgel liquids was analyzed by computing the one-dimensional mean squared displacement (MSD) along the x-coordinate direction against lag time, τ

$$\langle \Delta x^2 \rangle = \langle [\frac{1}{N}] \sum_{j=1}^{N} \quad x_j(t) \quad x_j(\tau) \ ^2 \tag{2}$$

which is averaged over all the N particles in the scan area of the middle layer across two surfaces and initial time, t.[5,39]

■ RESULTS AND DISCUSSION

We start with examining the effect of spatial confinement on the dynamics of highly deformable PNIPAM microgel liquid of E_p = 169 Pa at apparent volume fractions, ϕ = 0.49. ϕ is calculated based on the undeformed microgel hydrodynamic diameter, d_H = 1.4 ± 0.05 μm, measured in the dilute suspension limit of ϕ < 0.40 for PNIPAM microgels.[32] According to the previously reported phase diagram of bulk PNIPAM suspensions against ϕ and E_p,[32] PNIPAM microgels of E_p = 169 Pa exhibit a typical liquid behavior at ϕ = 0.49. We quantify the effect of spatial confinement on the particle mobility of PNIPAM microgel liquids by one-dimensional x-component MSD using eq 2. We choose not to analyze the MSD along the z-direction due to insufficient temporal resolution, which has been commonly neglected in microscopic studies of colloidal dynamics.[5,28,29,40] On the other hand, the resolution in the x and y directions for acquired confined particles in the middle layer between two surfaces is equivalent, and therefore $\langle \Delta x^2 \rangle \approx \langle \Delta y^2 \rangle$, which has been confirmed previously with confined "hard-sphere"-like colloidal liquids.[5,28,29] Figure 1a shows the H/d_H-dependent $\langle x^2 \rangle$ for confined PNIPAM microgel liquids of ϕ = 0.49, where H is the confinement gap spacing as determined by the travel distance of the fine micrometer and confirmed by z-directional gap depth by CLSM. Surprisingly, PNIPAM microgels show nearly no change in the MSD as the gap spacing is reduced from the bulk to H/d_H = 11, exhibiting little impact of spatial confinement on the dynamics of highly deformable microgel particles. We have fitted the linear region in longer τ, where the slope α = 1 by $\langle \Delta x^2 \rangle = 2Dt^\alpha$, and obtained the diffusion coefficient, D = 0.42 $\mu m^2/s$, which agrees well with the calculated D = 0.35 $\mu m^2/s$ based on the Stokes equation, $D = k_B T/6\pi\eta R$ with known water viscosity, η, at T = 298 K and microgel radius, R (=0.70 μm), within experimental uncertainty. Thus, it indicates that the diffusive dynamics of confined microgel particles in aqueous liquid media is preserved even down to H/d_H = 11, confirming bulk liquid behaviors. In control, we also examine the MSD of the "hard-sphere"-like PNIPAM microgel of E_p = 22 kPa at the same ϕ = 0.49 as shown in Figure 1b. Confinement-induced dynamic arrest of confined noncompliant microgels is clearly observed: the measured MSD is reduced by more than 1−2 orders of magnitude from that of the bulk liquid (at typically H/d_H >85−100) as H/d_H is decreased from ∼43 to 21 or smaller, which is in sharp contrast to that of the confined PNIPAM microgel of E_p = 169 Pa at similar H/d_H. At the smallest H/d_H, dynamic arrest of confined PNIPAM particles is exhibited with a plateau in the MSD, indicating dynamic arrest without net displacement over a considerably long lag time.[5] Such a strong confinement effect on the mobility of the PNIPAM microgel of E_p = 22 kPa is consistent with previously reported confine-

https://doi.org/10.1021/acs.langmuir.1c00363
Langmuir XXXX, XXX, XXX−XXX

ment-induced glassy dynamics of "hard-sphere" colloidal liquids.[5,28,29] In comparison, the contrasting results shown in Figure 1a,b clearly indicate a distinct confinement effect on the dynamics of compliant microgels from that of noncompliant ones. Intriguingly, spatial confinement appears to exhibit a considerably weak impact on the dynamics of highly deformable microgel liquids.

To further understand the dynamic response of highly deformable microgel liquids to spatial confinement, we also analyze the particle mobility of the confined PNIPAM microgel of E_p = 169 Pa at high ϕ = 0.56 and 0.70, at the latter of which bulk microgel liquids exhibit supercooled glass-like dynamic behaviors.[32,34] The reduction of measured MSD at ϕ = 0.56 and 0.70 from that of ϕ = 0.49 for bulk microgel liquids (at H/d_H >85−100) agrees well with the previous MSD results simply due to the well-known ϕ-effect.[32] As shown in Figure 2, as H/d_H is reduced to be smaller than 20 particle layers, particle mobility of microgel liquids at both ϕ = 0.56 and 0.70 commences to slowdown. A moderate reduction by a factor of 3−5 from the bulk mobility is observed at H/d_H = 16 and 22 at ϕ = 0.56 and 0.70, respectively. At further lesser gap spacings, a narrow plateau in MSD emerges at H/d_H = 14 for ϕ = 0.70, suggesting the confinement effect on microgel dynamic arrest. Apparently, the plateau in MSD of confined PNIPAM microgels of E_p = 169 Pa in Figure 2 is much narrower over a short lag time than that observed with the confined microgel of E_p = 22 kPa at ϕ = 0.49 (Figure 1b) and ϕ = 0.56 (Supporting Information Figure S2). In sharp contrast, significant dynamic arrest over a much longer lag time period of up to 1000 s is observed with the confined microgel of E_p = 22 kPa at ϕ = 0.56 as shown in Supporting Information Figure S2, suggesting a confinement-induced glassy behavior of confined "hard-sphere" liquid. Conversely, the results in Figure 2 suggest that confined deformable microgels of E_p = 169 Pa mostly remain uncaged from their neighbors and exhibit a very liquid-like behavior. Thus, for PNIPAM microgels of E_p = 169 Pa, the MSD results at three different ϕ_s values as shown in Figures 1a and 2a,b strongly indicate that spatial confinement exhibits a much weaker effect on their dynamics than that of the PNIPAM microgel of E_p = 22 kPa as well as model "hard-sphere" colloidal liquids.[5,28,29]

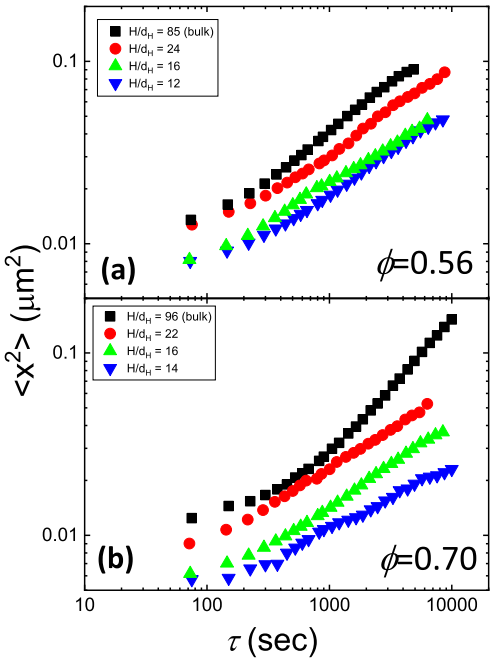

Figure 2. MSD against lag time for confined PNIPAM microgel liquids of E_p = 169 Pa at ϕ = (a) 0.56 and (c) 0.70 at varied gap spacings, H/d_H, as denoted in each panel.

To seek the answer for a much weakened effect of spatial confinement on the dynamics of PNIPAM microgels of low compliance, we investigate the structure and size change of confined microgels of E_p = 169 Pa by analyzing their pair correlation function, $g(r)$, against H/d_H. Figure 3a−c shows the H/d_H-dependent $g(r)$ of PNIPM microgels of E_p = 169 Pa at ϕ = 0.49, 0.56, and 0.70, respectively. At ϕ = 0.49, the first peak of $g(r)$ of the confined PNIPAM microgel liquid shows no shift in the interparticle separation distance or a clear change in its intensity down to the smallest gap spacing of H/d_H = 11 as allowed in this work. It is similar to the $g(r)$ of the confined PNIPAM microgel of E_p = 22 kPa and the same ϕ = 0.49 as shown in Supporting Information Figure S3. In contrast, for confined PNIPM microgels of E_p = 169 Pa at ϕ = 0.56 and 0.70, the first peak of $g(r)$ clearly shifts to smaller r when the gap spacing is reduced to H/d_H = 12 and 22 as shown in Figure 3b,c, respectively. At ϕ = 0.70, the first peak shifts to further smaller r upon decreasing H/d_H from 22 to 16 and 14. Yet, no clear enhancement in the peak values is observed at both ϕ_s. Thereby, it is suggested that spatial confinement imposes a nearly negligible structuring effect on highly deformable microgels, except their size, even when H/d_H is reduced to be approximately 10 particle layer thickness, distinct from strong wall-induced layering with confined "hard-sphere" liquids.

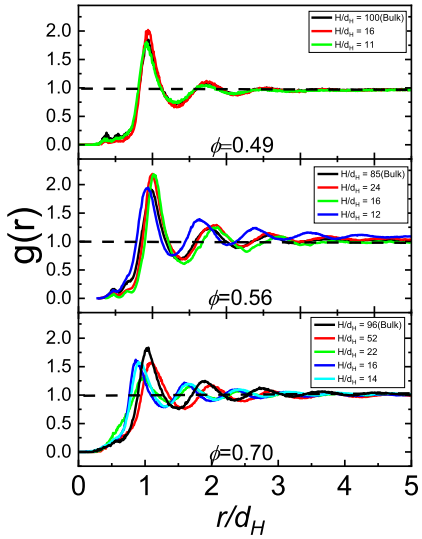

Figure 3. Pair correlation function, $g(r)$, of confined PNIPAM microgel liquids of E_p = 169 Pa between two solid surfaces of varied gap spacings, H/d_H, at ϕ = (a) 0.49, (b) 0.56, and (c) 0.70.

According to $g(r)$ as shown in Figure 3, the effect of spatial confinement on the effective diameter, d_{eff}, of PNIPAM microgel particles of E_p = 169 Pa and varied ϕ is summarized against H/d_H in Figure 4. At ϕ = 0.49, confinement causes a negligible change in the size of PNIPAM microgels down to the smallest gap spacing of H/d_H = 11. In comparison, 5−10% size reduction is observed with confined microgel liquids at ϕ = 0.56 and 0.70. Confinement-induced size reduction could

https://doi.org/10.1021/acs.langmuir.1c00363
Langmuir XXXX, XXX, XXX−XXX

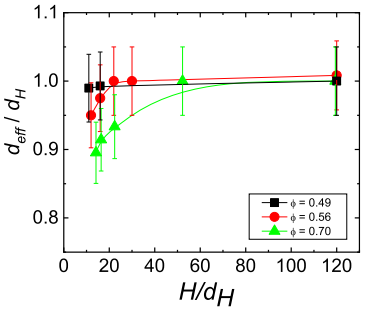

Figure 4. Effective particle diameter, d_{eff}, normalized by the hydrodynamic diameter, d_H, of confined PINPAM microgel particles in aqueous suspensions of ϕ = 0.49 (squares), 0.56 (circles), and 0.70 (triangles) against H/d_H.

lead to an increase of the microgel effective volume fraction to 0.61 and 0.79 in comparison to their respective initial ϕ = 0.56 and 0.70. It is noted that despite a confinement-induced increase of effective ϕ at the smallest gap spacing, microgel liquids remain in the supercooled liquid phase, not in the glass phase that is reported to occur at $\phi \geq 0.87$.[32] Combined with H/d_H-dependent $g(r)$, the results suggest that the moderate size reduction of confined deformable microgels could be attributed to the structural disruption of microgel particles near the confining surfaces, leading to the preserved liquid-like structure and unimpeded dynamics of microgel liquids even down to strong spatial confinement.

With strong evidence of nearly unimpeded particle mobility of confined highly deformable microgel liquids, it is also of great interest to determine how confinement influences structural relaxation. We thereby analyze the overlapping order parameter

$$q_s(\tau) = \frac{1}{N}\sum_{i=1}^{N} w(|r_i(\tau) \quad r_i(\theta)|) \qquad (3)$$

where w = 1 or 0 if $|r_i(\tau) - r_i(0)|$ ⟨or⟩ a, respectively. $q_s(\tau)$ quantifies the average number of "overlapping" particles separated by the distance, a, over a given τ and has been employed in the study of glassy dynamics of dense liquids and confined thin film.[29] For confined highly compliant microgels, we are interested in the impact of gap spacing on the localization of deformable particles. In $q_s(\tau)$, the parameter a is a "coarse graining" length scale that is typically larger than the vibration amplitude of particle motion in the β-regime. For model "hard-sphere" liquids, the particle radius is often chosen as a to give the best distinction between the localized and delocalized particles.[29] In this work, considering the deformation and size change of microgel particles with decreasing gap spacing, we approximate a to the first peak of $g(r)$ at given ϕ and H/d_H as determined in Figure 3. Considering that no evident effect of spatial confinement is observed with the PNIPAM microgel of E_p = 169 Pa at ϕ = 0.49 (see Supporting Information Figure S4), we merely focus on analyzing $q_s(\tau)$ at ϕ = 0.56 and 0.70 as shown in Figure 5a,b, respectively. At larger H/d_H, a rapid α-relaxation process is observed to resemble the typical liquid behaviors. Moderate slowdown of the structural relaxation process is observed with the shift of $q_s(\tau)$ to longer τ when the gap spacing is reduced. However, it is noted that at the smallest gap spacing, H/d_H = 12−16 at both ϕ, no clear dynamic trapping is observed in sharp contrast to the plateau observed for the confined

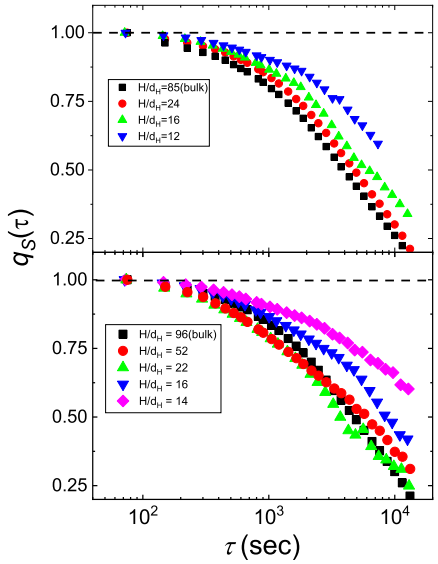

Figure 5. Overlap order parameter, $q_s(\tau)$, of the confined PNIPAM microgel liquid of E_p = 169 Pa at ϕ = (a) 0.56 and (c) 0.70 at varied gap spacings, H/d_H, as denoted in each panel.

PNIPAM microgel of E_p = 22 kPa at ϕ = 0.49 and H/d_H = 9 (see Supporting Information Figure S5) or the previously reported for confined hard-sphere liquids.[29,30]

Accordingly, we extract the α-relaxation time, τ_α, which characterizes the superexponential decay of $q_s(\tau)$, by fitting $q_s(\tau)$ with the Kohlrausch−Williams−Watts (KWW) formula

$$q_s(\tau) = A \exp(-(\tau/\tau_\alpha)^\beta) \qquad (4)$$

where A is a freely floating parameter and β is the stretching exponent.[30,41] Normalized τ_α by the relaxation time in the bulk (H/d_H >100), $\tau_{\alpha,\,bulk}$, for the confined PNIPAM microgel of E_p = 169 Pa at ϕ = 0.56 and 0.70 is plotted against H/d_H in Figure 6. At ϕ = 0.70, τ_α exhibits a gradual growth from ∼5000 s to

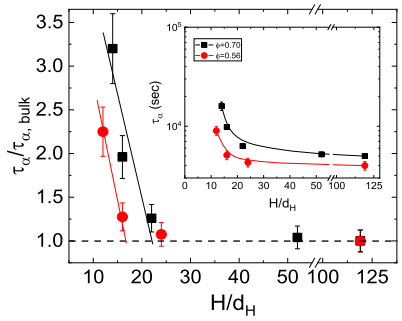

Figure 6. Normalized α-relaxation time, τ_α, by $\tau_{\alpha,bulk}$ of the confined PNIPAM microgel liquid at ϕ = 0.56 (red circles) and 0.70 (black squares) against H/d_H. The interception of the extrapolation of $\tau_\alpha/\tau_{\alpha,\,bulk}$ at small H/d_H with unity determines $(H/d_H)_{cr}$. Inset: H/d_H-dependent τ_α.

∼6300 s and ∼10,000 s as H/d_H is decreased from 52 to 22 and 16, respectively. A similar behavior is observed at ϕ = 0.56: τ_α increases from ∼4000 s to ∼9500 s when H/d_H is decreased from 24 to 12. In this work, τ_α for confined highly deformable microgel even down to the smallest H/d_H ∼12 is far smaller than the measured α-relaxation time, $\tau_{\alpha,glass}$ ≈10,000 s, for the same microgel in the bulk glass phase at ϕ_g = 0.87,[32] thus no

https://doi.org/10.1021/acs.langmuir.1c00363
Langmuir XXXX, XXX, XXX−XXX

glass transition is induced by strong spatial confinement, distinct from the confinement effect on model "hard-sphere" colloidal liquids at the similar volume fractions. We estimate the critical gap spacing, $(H/d_H)_{cr}$, for the onset of the confinement effect when τ_α deviates from $\tau_{\alpha,bulk}$, that is, $\tau_\alpha/\tau_{\alpha,bulk} \approx 1$ based on the interception in gap spacing from the linear extrapolation of $\tau_\alpha/\tau_{\alpha,bulk}$ to the unity as illustrated in Figure 6. We therefore determine $(H/d_H)_{cr}$ for the highly deformable PNIPAM microgel of E_p = 169 Pa to be approximately 16 and 22 at ϕ = 0.56 and 0.70, respectively, while $(H/d_H)_{cr}$ for ϕ = 0.49 cannot be accessed experimentally due to the limit of the smallest gap spacing allowed in this work. However, it is noted that τ_α at ϕ = 0.49 remains nearly unchanged even when H/d_H is reduced down to 11, it is thus reasonable to derive that $(H/d_H)_{cr}$ for the microgel at ϕ = 0.49 must be smaller than 10. In comparison, according to the H/d_H-dependent τ_α for confined microgels of E_p = 22 kPa at ϕ = 0.49 (see Supporting Information Figures S2 and S3), $(H/d_H)_{cr}$ is determined to be approximately 25, smaller than the reported $(H/d_H)_{cr}$ = 40−58 that leads to the glass behavior of confined model "hard-sphere" liquids at ϕ = 0.43−0.57.[30] Cautiously, by taking the confinement-induced change of d_{eff} into consideration, we estimate the error of $(H/d_H)_{cr}$ could be roughly 2−3 particle layers given by 5% reduction of d_{eff}. Nevertheless, the obtained $(H/d_H)_{cr}$ <10, ∼16 ± 2, and ∼22 ± 2 for the highly deformable PNIAPM microgel of E_p = 169 Pa at ϕ = 0.49, 0.56, and 0.70, respectively, is much smaller than $(H/d_H)_{cr}$ ∼ 25 for the PNIPAM microgel of E_p = 22 kPa and ϕ = 0.49 (Supporting Information Figure S6) as well as ∼40−58 for model "hard-sphere" colloidal liquids at equivalent or lower ϕ as reported previously.[5,28,30] Hence, all the results suggest that spatial confinement exhibits a considerably weak impact on highly compliant microgel liquids. Particle deformation under confinement could be attributed to facilitate structural relaxation of confined microgel liquids, where deformation-induced dynamic interaction between microgel particles could lead to the delay in confinement-induced dynamic retardation.

■ CONCLUSIONS

In summary, we have experimentally demonstrated that spatial confinement exhibits a much weaker effect on the structural dynamics of highly compliant PNIPAM microgel liquids than that of stiff PINIAM microgel liquids of the same chemistry and similar volume fractions. The dynamics of the confined deformable microgel liquid of E_p = 169 Pa at ϕ = 0.49 highly resembles its bulk behavior down to the strongest confinement of H/d_H = 11, which approximates to the smallest gap spacing allowed in this experimental study. At increased ϕ = 0.56 and 0.70, we have observed a marginal decrease by a factor of 3−5 in particle mobility of confined microgel liquids when H/d_H is reduced below 20. In sharp contrast, the confined stiff PNIPAM microgel of E_p = 22 kPa at ϕ = 0.49 and 0.56 exhibits significant dynamic arrest upon decreasing H/d_H from ∼43 to ∼21, where the particle mobility is reduced by 1−2 orders of magnitude. Based upon H/d_H-dependent τ_α, $(H/d_H)_{cr}$, which indicates the onset of spatial confinement effect on microgel dynamics, is determined based on the deviation of $\tau_\alpha/\tau_{\alpha,bulk}$ from the unit and approximates to 17 and 22 for the deformable PNIPAM microgel of E_p = 169 Pa at ϕ = 0.56 and 70, respectively. Apparently, $(H/d_H)_{cr}$ for a highly compliant PNIPAM microgel even at higher ϕ is smaller than those of stiff PNIPAM microgels at ϕ = 0.49 or the reported $(H/d_H)_{cr}$ = 40−58 for model "hard-sphere" colloidal liquids at similar ϕ. Additionally, we have found that decreasing the gap spacing between two solid surfaces leads to the deformation and size shrinkage of PNIPAM microgel particles of E_p = 169 Pa at ϕ = 0.56−70, but not so with the microgel of E_p = 22 kPa. However, no apparent confinement-induced packing and ordering is observed with deformable microgels based on $g(r)$ analysis. Thus, it is suggested that confinement-induced particle deformation and resulting dynamic interparticle interaction could further frustrate particle packing and thereby facilitate structural relaxation of confined deformable microgels. Hence, the results in this work provide further insights into the correlation among material compliance, structural relaxation, and critical confinement gap spacing of complex polymeric liquids, which could become an effective and practical control of interfacial fluid transport and lubrication. In perspective, a future study of confined microgels of systematically varied particle compliance and the effect of confining surface compliance on confined liquids will be of great interest to seek optimal liquid and surface compliance for ultralow friction and superior lubrication.

■ ASSOCIATED CONTENT

Supporting Information

The Supporting Information is available free of charge at https://pubs.acs.org/doi/10.1021/acs.langmuir.1c00363.

Additional information on the experimental setup of confocal compressive apparatus, additional experimental results of confined "hard-sphere"-like microgel liquids at varied gap spacings, and gap spacing-dependent overlapping order parameter of a confined highly deformable microgel liquid at a low volume fraction of 0.49 (PDF)

■ AUTHOR INFORMATION

Corresponding Author

Yingxi Zhu − *Department of Chemical Engineering and Materials Science, Wayne State University, Detroit, Michigan 48202, United States*; orcid.org/0000-0002-7968-1640; Email: yzhu3@wayne.edu

Authors

Raymond P. Seekell, III − *LiquiGlide, Inc., Cambridge, Massachusetts 02139, United States*

Kehua Lin − *Department of Chemical Engineering and Materials Science, Wayne State University, Detroit, Michigan 48202, United States*

Complete contact information is available at: https://pubs.acs.org/10.1021/acs.langmuir.1c00363

Notes

The authors declare no competing financial interest.

■ ACKNOWLEDGMENTS

The authors acknowledge the financial support from the National Science Foundation (NSF CMMI-1761418) for this work.

■ REFERENCES

(1) McKenna, G. B. Ten (or more) years of dynamics in confinement: Perspectives for 2010. *Eur. Phys. J.* **2010**, *189*, 285−302.

(2) Alcoutlabi, M.; McKenna, G. B. Effects of confinement on material behaviour at the nanometre size scale. *J. Phys.: Condens. Matter* **2005**, *17*, R461−R524.

(3) Riggleman, R. A.; Yoshimoto, K.; Douglas, J. F.; Pablo, J. J. d. Influence of confinement on the fragility of antiplasticized and pure polymer films. *Phys. Rev. Lett.* **2006**, *97*, 045502.
(4) Roth, C. B.; Torkelson, J. M. Selectively Probing the Glass Transition Temperature in Multilayer Polymer Films: Equivalence of Block Copolymers and Multilayer Films of Different Homopolymers. *Macromolecules* **2007**, *40*, 3328−3336.
(5) Sarangapani, P. S.; Zhu, Y. Impeded structural relaxation of a hard-sphere colloidal suspension under confinement. *Phys. Rev. E: Stat., Nonlinear, Soft Matter Phys.* **2008**, *77*, 010501.
(6) Coudert, F.-X. Water Adsorption in Soft and Heterogeneous Nanopores. *Acc. Chem. Res.* **2020**, *53*, 1342−1350.
(7) Nazari, M.; Davoodabadi, A.; Huang, D.; Luo, T.; Ghasemi, H. Transport Phenomena in Nano/Molecular Confinements. *ACS Nano* **2020**, *14*, 16348−16391.
(8) Zhou, H.-X.; Rivas, G.; Minton, A. P. Macromolecular Crowding and Confinement: Biochemical, Biophysical, and Potential Physiological Consequences. *Annu. Rev. Biophys.* **2008**, *37*, 375−397.
(9) Ding, Y.; Ro, H. W.; Germer, T. A.; Douglas, J. F.; Okerberg, B. C.; Karim, A.; Soles, C. L. Relaxation Behavior of Polymer Structures Fabricated by Nanoimprint Lithography. *ACS Nano* **2007**, *1*, 84−92.
(10) Harrer, J.; Rey, M.; Ciarella, S.; Löwen, H.; Janssen, L. M. C.; Vogel, N. Stimuli-Responsive Behavior of PNiPAm Microgels under Interfacial Confinement. *Langmuir* **2019**, *35*, 10512−10521.
(11) Gong, X.; Li, L. Nanometer-Thick Ionic Liquids as Boundary Lubricants. *Adv. Eng. Mater.* **2018**, *20*, 1700617.
(12) Kienle, D. F.; Kuhl, T. L. Density and Phase State of a Confined Nonpolar Fluid. *Phys. Rev. Lett.* **2016**, *117*, 5.
(13) Khan, S. H.; Matei, G.; Patil, S.; Hoffmann, P. M. Dynamic Solidification in Nanoconfined Water Films. *Phys. Rev. Lett.* **2010**, *105*, 4.
(14) Jabbarzadeh, A.; Harrowell, P.; Tanner, R. I. The structural origin of the complex rheology in thin dodecane films: Three routes to low friction. *Tribol. Int.* **2007**, *40*, 1574−1586.
(15) Zhu, Y.; Granick, S. Reassessment of Solidification in Fluids Confined between Mica Sheets. *Langmuir* **2003**, *19*, 8148−8151.
(16) Krim, J. Friction and energy dissipation mechanisms in adsorbed molecules and molecularly thin films. *Adv. Phys.* **2012**, *61*, 155−323.
(17) Khan, S. H.; Kramkowski, E. L.; Ochs, P. J.; Wilson, D. M.; Hoffmann, P. M. Viscosity of a nanoconfined liquid during compression. *Appl. Phys. Lett.* **2014**, *104*, 023110.
(18) Atarod, M.; Ludwig, T. E.; Frank, C. B.; Schmidt, T. A.; Shrive, N. G. Cartilage boundary lubrication of ovine synovial fluid following anterior cruciate ligament transection: a longitudinal study. *Osteoarthritis Cartilage* **2015**, *23*, 640−647.
(19) Lee, D. W.; Banquy, X.; Israelachvili, J. N. Stick-slip friction and wear of articular joints. *Proc. Natl. Acad. Sci. U.S.A.* **2013**, *110*, E567−E574.
(20) Greene, G. W.; Banquy, X.; Lee, D. W.; Lowrey, D. D.; Yu, J.; Israelachvili, J. N. Adaptive mechanically controlled lubrication mechanism found in articular joints. *Proc. Natl. Acad. Sci. U.S.A.* **2011**, *108*, 5255−5259.
(21) Caligaris, M.; Ateshian, G. A. Effects of sustained interstitial fluid pressurization under migrating contact area, and boundary lubrication by synovial fluid, on cartilage friction. *Osteoarthritis Cartilage* **2008**, *16*, 1220−1227.
(22) Han, Y.; Shokef, Y.; Alsayed, A. M.; Yunker, P.; Lubensky, T. C.; Yodh, A. G. Geometric frustration in buckled colloidal monolayers. *Nature* **2008**, *456*, 898−903.
(23) Liu, Y.; Lorusso, D.; Holdsworth, D. W.; Poepping, T. L.; de Bruyn, J. R. Effect of confinement on the rheology of a yield-stress fluid. *J. Non-Newtonian Fluid Mech.* **2018**, *261*, 25−32.
(24) Geske, J.; Drossel, B.; Vogel, M. Structure and dynamics of a silica melt in neutral confinement. *J. Chem. Phys.* **2017**, *146*, 134502.
(25) Xie, S.-J.; Qian, H.-J.; Lu, Z.-Y. Hard and soft confinement effects on the glass transition of polymers confined to nanopores. *Polymer* **2015**, *56*, 545−552.
(26) Seth, J. R.; Locatelli-Champagne, C.; Monti, F.; Bonnecaze, R. T.; Cloitre, M. How do soft particle glasses yield and flow near solid surfaces? *Soft Matter* **2012**, *8*, 140−148.
(27) Alba-Simionesco, C.; Dosseh, G.; Dumont, E.; Frick, B.; Geil, B.; Morineau, D.; Teboul, V.; Xia, Y. Confinement of molecular liquids: Consequences on thermodynamic, static and dynamical properties of benzene and toluene. *Eur. Phys. J. E: Soft Matter Biol. Phys.* **2003**, *12*, 19−28.
(28) Nugent, C. R.; Edmond, K. V.; Patel, H. N.; Weeks, E. R. Colloidal Glass Transition Observed in Confinement. *Phys. Rev. Lett.* **2007**, *99*, 025702.
(29) Sarangapani, P. S.; Schofield, A. B.; Zhu, Y. Direct experimental evidence of growing dynamic length scales in confined colloidal liquids. *Phys. Rev. E: Stat., Nonlinear, Soft Matter Phys.* **2011**, *83*, 030502.
(30) Sarangapani, P. S.; Schofield, A. B.; Zhu, Y. Relationship between cooperative motion and the confinement length scale in confined colloidal liquids. *Soft Matter* **2012**, *8*, 814−818.
(31) Richert, R. Geometrical confinement and cooperativity in supercooled liquids studied by solvation dynamics. *Phys. Rev. B* **1996**, *54*, 15762−15766.
(32) Seekell, R. P., III; Sarangapani, P. S.; Zhang, Z.; Zhu, Y. Relationship between particle elasticity, glass fragility, and structural relaxation in dense microgel suspensions. *Soft Matter* **2015**, *11*, 5485−5491.
(33) Lindsay, H. M.; Chaikin, P. M. Elastic properties of colloidal crystals and glasses. *J. Chem. Phys.* **1982**, *76*, 3774−3781.
(34) Mattsson, J.; Wyss, H. M.; Fernandez-Nieves, A.; Miyazaki, K.; Hu, Z.; Reichman, D. R.; Weitz, D. A. Soft colloids make strong glasses. *Nature* **2009**, *462*, 83−86.
(35) Pelton, R. H.; Chibante, P. Preparation of aqueous latices with N-isopropylacrylamide. *Colloids Surf.* **1986**, *20*, 247−256.
(36) Yang, J.; Schweizer, K. S. Glassy dynamics ad mechanical response in dense fluids of soft repulsive spheres. I. Activated relaxation, kinetic vitrification and fragility. *J. Chem. Phys.* **2011**, *134*, 204908.
(37) Crocker, J. C.; Grier, D. G. Methods of digital video microscopy for colloidal studies. *J. Colloid Interface Sci.* **1996**, *179*, 298.
(38) Weeks, E. R.; Crocker, J. C.; Levitt, A. C.; Schofield, A.; Weitz, D. A. Three-dimensional direct imaging of structural relaxation near the colloidal glass transition. *Science* **2000**, *287*, 627−631.
(39) Yamamoto, R.; Onuki, A. Dynamics of highly supercooled liquids: Heterogeneity, rheology and diffusion. *Phys. Rev. E: Stat., Nonlinear, Soft Matter Phys.* **1998**, *58*, 3515.
(40) Weeks, E. R.; Weitz, D. A. Properties of cage rearrangements observed near the colloidal glass transition. *Phys. Rev. Lett.* **2002**, *89*, 095704.
(41) Liétor-Santos, J. J.; Sierra-Martín, B.; Fernández-Nieves, A. Bulk and shear moduli of compressed microgel suspensions. *Phys. Rev. E: Stat., Nonlinear, Soft Matter Phys.* **2011**, *84*, 060402.

https://doi.org/10.1021/acs.langmuir.1c00363
Langmuir XXXX, XXX, XXX−XXX